Celal Bayar University Journal of Science

Filler Type and Particle Distribution Effect on Some Properties of Polymer Composites

Bayram Poyraz[1], Şevki Eren[2*], Serkan Subaşı[3]

[1]Duzce University, Faculty of Technology, Department of Civil Engineering, Düzce, 81620, Turkey
[2*]Kırşehir Ahi Evran University, Vocational School, Department of Construction Technology, Kırşehir, Turkey
[3]Duzce University, Faculty of Technology, Department of Civil Engineering, Düzce, 81620, Turkey
*seren@ahievran.edu.tr
* Orcid:0000-0003-0773-4034

Received: 1 September 2020
Accepted: 1 March 2021
DOI: 10.18466/cbayarfbe.787883

Abstract

This study reports the effects of silica (S), quartz (Q), and basalt (B) fillers on the chemical, thermal, and mechanical properties of unsaturated polyester (PE) composites. In the study, fillers were selected as same class grain distribution and mixed with orthophtalic based PE resin to produce composites. The thermal characterization of the composites was determined with thermogravimetric and thermal conductivity. Chemical characterization was carried out with FT-IR. Compressive strength was investigated with Universal Testing Machine. SEM device was used to investigate the morphological alterations of the composites. Also, statistical analysis was carried out for thermal conductivity and mechanical results. At the end of the present study, some minor chemical alterations were seen in FT-IR after the interaction of the fillers and PE resin. Thermal stability decreased after adding fillers. The thermal conductivity and thermogravimetric analysis were not agreed with each other that higher thermal conductivity was seen in the PE-Q composites. The compressive strength of filler-based composites was higher than that of the neat PE composite whereas the higher compressive strength was obtained in the PE-Q. This study confirms the applicability of various fillers as a reinforcing agent in the polymer.

Keywords: Compressive strength, FT-IR, Grain distribution, Polymer composites, SEM, Silica, quartz and basalt fillers, Thermogravimetric and thermal conductivity.

1. Introduction

Composites were mostly used as a substitute for conventional materials due to the revealing high strength at a small specific weight, high rigidity as well as the ability to be tailored for specific purposes [1-4].
PE having doubled bonds and giving crosslinking are mainly used in the production of the composites for any applications due to the ease of use and the low cost easily tailoring of the mechanical and chemical properties. Several phenomena were carried out to improve the performance of PE polymers. One of the traditional methods is the pooling of a PE with inorganic substances through physical or weak phase interaction e.g., hydrogen bonding, van der Waals forces, or strong covalent bond e.g., between the organic and inorganic phases. In this way, organic-inorganic composites combine the ductility, flexibility, resistance, thermal stability, rigidity, and dielectric of their distinct properties [5-8].

Inorganic fillers are a promising reinforcing agent in the modification of polymers that if the inorganic fillers having different dimensions of a dispersed phase in PE composite would alter mechanical and thermal properties that cannot be obtained with traditional PE composites. Because fillers restrict the movement of the polymer chain and increase the formability of the material. With those properties, tensile strength, hardness, abrasion resistance, rigidity, the toughness of the composites can be improved [9-11].

Mahdi et al. [12] studied PET obtaining from waste bottles. In this study, they used methyl ethyl ketone peroxide (MEKP) and cobalt naphthenate (CoNp) as free radical initiator and the catalyst, respectively. Afterward, they mixed with inorganic aggregate (10% w/w. aggregate/resin). The maximum compressive strength was measured as 42.2 MPa that this obtained value is higher than those of the compressive strength of the neat polymer composite (28.5 MPa). Ateş and Barnes [13] prepared polymer concrete composite

specimens by using polyester and quartz as binder and filler material, in different aggregate diagrams and binder ratio. The highest compression strength was obtained as 95.8 MPa. Ateş [14] examined the change of the compressive strength properties of the polyester and epoxy resin-based composite material having quartz sand as a filler which has different grain distributions and produced by using binder material at different ratios. The highest compressive strength value was obtained as 62.8 MPa in a mixture of 18% resin + 82% quartz filler. Singh et al. [15] fabricated silica-polyester composites having 0.5-2.5% by weight in the presence of cobalt octoate and MEKP via the compression molding method cured for 24 h at room temperature. The tensile yield strength and tensile modulus increased with the filler content from 10.58 MPa to 25. 99 MPa, and 1.11 GPa to 1.61 GPa for sheets containing 1.5 % colloidal silica filler content. After that point, there is a substantial decrease in the tensile modulus. Flexural strength and flexural modulus revealed a similar trend with increasing filler content as tensile properties did. That probably stems from good newly bonding and uniform dispersion of the smaller size of particles. The increase in filler content caused new bonds in the resin matrix. Besides, agglomeration which reduces the strength of the composites occurred as well.

The objective of this study was to investigate how particle size distribution and type of filler influence the chemical, thermal and mechanical properties of the composites. For that purpose, silica, quartz, and basalt fillers were embedded in unsaturated ortophthalic polyester resins. Then, polyester resins were cured in certain conditions with methyl ethyl ketone peroxide (initiator) in the presence of cobalt octoate (catalyst) to obtain polyester-filler composites. After production, FTIR, thermogravimetric analysis, thermal conductivity, and mechanical analysis were carried out.

2. Materials and Methods

2.1. Matrix Materials

In this study, the orthophtalic acid resin was used as a thermosetting composite matrix (1.12 g/cm3, 66% solid content, Polipol 3562-SR, Turkey) and MEKP (ER 59, Akperox, Turkey) and cobalt octoate (RC88, Akkobalt, Turkey) was used as initiator and catalyst, respectively. In the study, silica filler, quartz filler, and basalt filler were used in the 0-1000 µm grain size range in the composites.

2.2. Design of The Experiments

The orthophtalic acid resin having initiator and catalyst were mixed with fillers in certain conditions and those are classified as a polyester-silica filler (PE-S), polyester-basalt filler (PE-B), and polyester-quartz filler (PE-Q). Filler grain-size distribution was determined as Fuller equation. The reference "Fuller equation" is given in Equation 2.1 and in this equation, n=0.8 was taken as [16]. Filler grain-size distributions are represented in Figure 1.

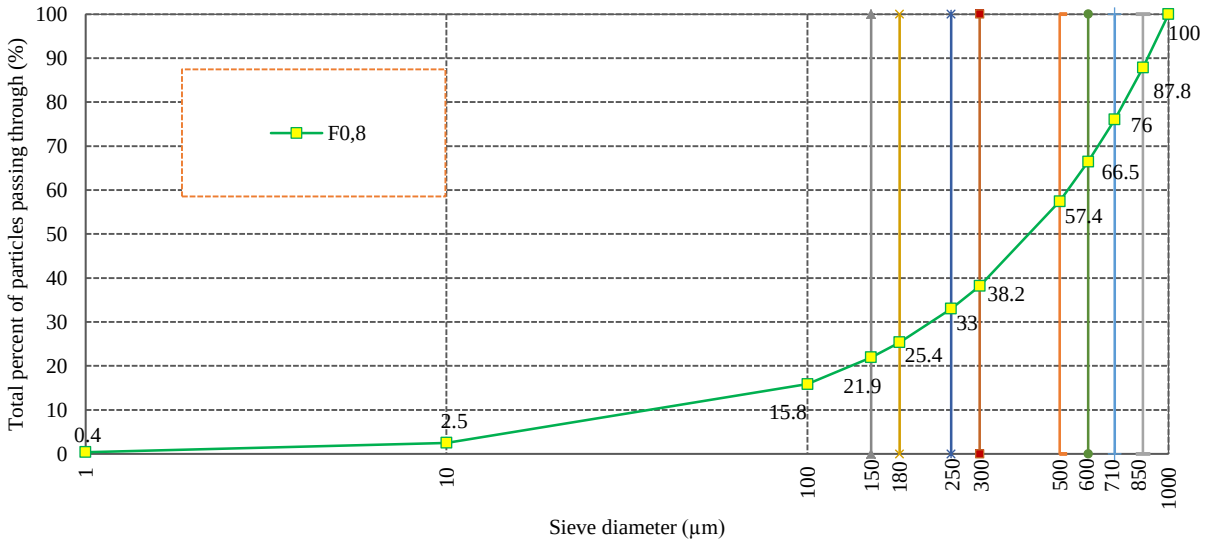

Figure 1. F 0.8 grain size distributions of the fillers

$$P\% = \left(\frac{d}{D}\right)^n \quad \textbf{(2.1)}$$

P%: total percent of particles passing through.
d: diameter of the current sieve (µm)
D: maximum size of aggregate (1000µm)
n: exponent of the equation (n=0.8)

Together with grain-size distribution, chemical and physical properties of the fillers are other parameters that affect the chemical, thermal and mechanical properties of the thermosetting composites. Chemical and physical parameters of the fillers are given in Table 1, and Table 2.

Table 1. Chemical compositions of filling materials.

Chemical Composition	Fillers (%)		
	Quartz	Silica	Basalt
Silicon Dioxide (SiO_2)	99.18	98.94	61.21
Aluminium Oxide (Al_2O_3)	LOD*	0.08	13.61
Iron Oxide (Fe_2O_3)	0.02	0.1	5.72
Magnesium Oxide (MgO)	LOD*	LOD*	3.9
Calcium Oxide (CaO)	0.16	LOD*	6.2
Sodium Oxide (Na_2O)	LOD*	LOD*	2.63
Potassium Oxide (K_2O)	0.03	0.05	2.83
Titanium Oxide (TiO_2)	0.04	0.12	0.76
Manganes (II) Oxide (MnO)	LOD*	LOD*	0.13
Sulphur Dioxide (SO_2)	0.02	0.3	LOD*
Diphospor pentaoxide (P_2O_5)	0.01	0.01	LOD*
Chrome (II) Oxide (Cr_2O_3)	0.004	0.053	LOD*
Manganes (III) Oxide Mn_2O_3	0.0017	0.004	LOD*

*LOD: Limit of Detection

Table 2. Physical test results of filling materials.

Physical parameters	Silica	Basalt	Quartz
Moisture content (%)	0.002	0.6	0.5
Burning loss (%)	1.3	2.6	1.2
Specific gravity (gr/cm^3)	2.55	2.74	2.57
Compact unit weight (gr/cm^3)	1.79	1.72	1.76
Loose unit weight (gr/cm^3)	1.62	1.53	1.54
Water absorption ratio (%)	2.03	2.73	2.29
Specific surface area (μ)	12.07	11.31	10.42

2.3. Composite Fabrication

The orthophtalic resin, methyl ethyl ketone peroxide, and cobalt octoate were added to the beaker with a volume ratio of 100:1:1, respectively. Afterward, the former mixture stirred 2 min at 300 rpm in the magnetic stirrer (Figure 2) and numbered experimental protocol in the manuscript.

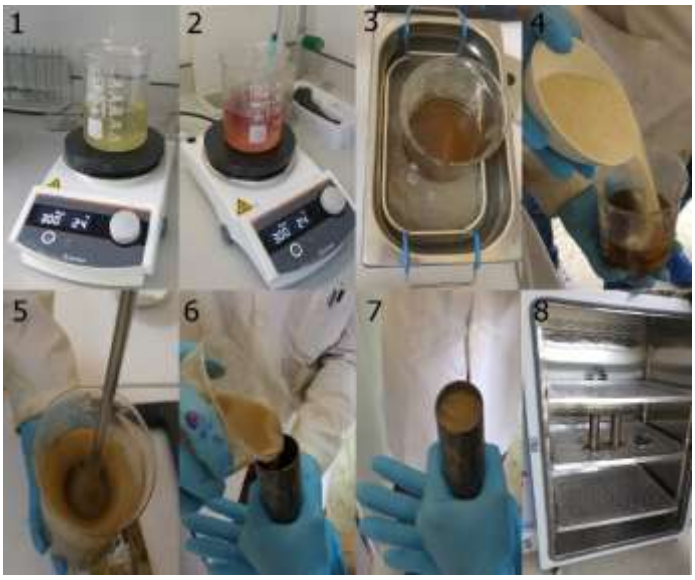

Figure 2. Experimental demonstration

Celal Bayar University Journal of Science
Volume 17, Issue 1, 2021, p 79-89
Doi: 10.18466/cbayarfbe.787883

1-2: Preparing resin and pouring the initiator on the orthophtalic resin
3: Mixing of the resin and additives in the sonicator
4: Adding of the filler
5: Mixing in the disperser
6-7: Pouring the mixture into the steel mold, and molding
8: Curing process
Before the curing, the former prepared solution was transferred to ultrasonic homogenizer (Bandelin, RK 100 H, Germany) and sonicated for 1 min at 35 kHz to improve the homogeneity. Then the obtained mixture was transferred and the fillers that prepared according to Fuller equation were added and mixed at 1000 rpm for 1 min in the ultraturrex disperser (Heidolph, Hei TORQUE 100, Germany) before the resin reached the gelling time. Finally, the obtained suspension poured for molding to a steel cylinder (3cm x 6 cm) with controlled leveling and kept at room temperature for 1h and afterward was transferred to an oven (Utest. UTD 1035, Turkey) to kept at 80 °C for 24h. Release agent (Poliya, Polivaks SV-6, Turkey) were applied to the molds to remove easily after curing. The production of silica (PE-S), quartz (PE-Q), and basalt (PE-B) filled polyester composites are given in Figure 3.

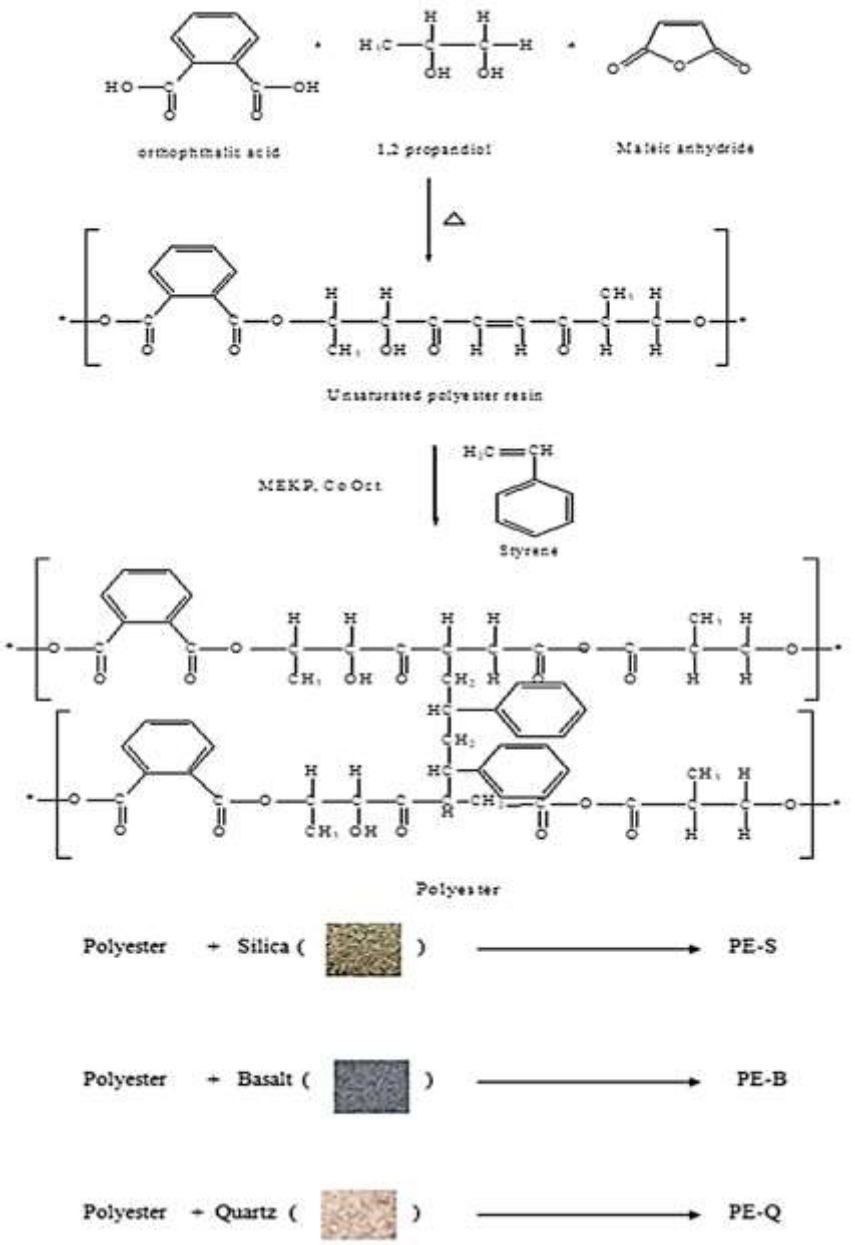

Figure 3. Production of silica (PE-S), quartz (PE-Q), and basalt (PE-B) filled polyester composites.

2.4. Polymerization Analysis (Chemical Analysis)

The IR spectra were taken via an attenuated total reflectance (ATR)-FTIR device (Shimadzu IR Prestige-21, Shimadzu Corp.). The samples were gently put in an attachment containing a diamond to evaluate molecular vibration signals in the range of 4000-600 cm-1, and 20 scans with a resolution of 4 cm-1 were carried out.

2.5. Thermogravimetric Analysis

Thermogravimetric analysis was performed on a DTG 60 (Shimadzu) analyzer equipped with a thermal analysis data station at a heating rate of 10 °C/min under a 75 mL/min nitrogen atmosphere. The materials were first dried at room temperature overnight. 5-10 mg of the material was placed in a platinum pan and heated from room temperature to 1200 °C. For SEM analysis, cross-section images were taken of the samples at 20 kV acceleration voltage (FEI, Quanta 250. Netherland). The specimens were mounted with tweezers onto a substrate with carbon tape and coated with a thin layer of gold/palladium mixture.

2.6. Thermal Conductivity Analysis

The thermal conductivity analysis, a sample having a smooth surface was prepared and put the specimen sensor, then 500 g weightiness was put over the sensor then applied current thoroughly 3 seconds and measurements are saved.

2.7. Compressive Test

After the samples were removed from the cylinder molds, they were subjected to a cutting process for pressure tests. After 7 days of waiting time, pressure tests were performed on the cut samples. The pressure test was performed according to ASTM C 579-01 [17]. Samples were produced in a cylindrical shape with a diameter to length ratio of ½ (35mm / 70mm). Loading speed, 41 MPa / min. is set to. In order to perform the pressure test, 3 samples were produced from each mixture.

3. Results and Discussion

3.1. Chemical Characterization

The FTIR spectra were investigated to determine molecular vibrations for all composites. The obtained spectra are given in Figure 4.

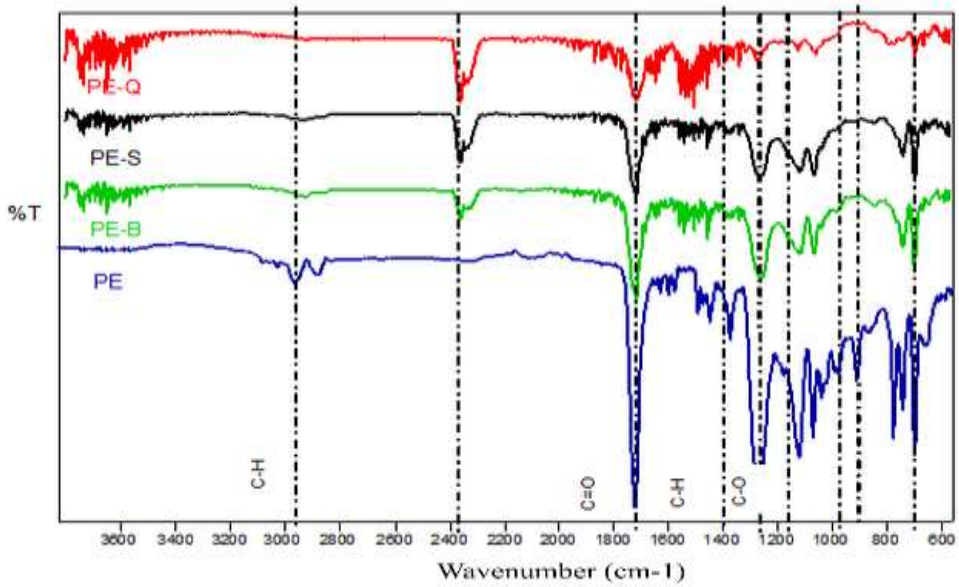

Figure 4. FTIR spectra of the PE, PE-S, PE-B, and PE-Q composites.

C-H asymmetric and symmetric stretching vibration of the methylene group found in the composites was observed at 2967 cm^{-1} [18]. However, this interaction was seen only in the PE composite. C=O stretching vibrations of the neat PE composite were observed at 1721 cm^{-1}. After the interaction of the PE and fillers, all of C=O vibration were approximately seen at 1716 cm^{-1}. C=C vibration that is related to C=C in the aromatic ring was observed at 1599 cm^{-1} for all composites. It was encountered C-H bending vibrations at 1494 cm^{-1} for the PE whereas this vibration saw at 1491 cm^{-1} for filled composites. Another, C-H bending vibrations were seen at 1259 cm^{-1}, 1261 cm^{-1}, 1269 cm^{-1} for the PE-B, PE-S, and PE-Q, respectively. The other vibration which is for the PE at 1121 cm^{-1} was seen at

1117 cm^{-1} for PE-S and 1118 cm^{-1} for PE-B. However, it was not observed in the PE-Q.

It seems that vibration is not related to Si-C or Si-O interaction as quartz and silica are comprised of mostly from SiO_2 molecules. Besides, as well as chemical shifts, alterations in the intensity were determined between PE and fillers. The intensity of PE vibrations was significantly decreased due to decreasing resin concentration in the composites. With a similar trend, the intensity of carboxyl groups (-C=O) found at 1721 cm^{-1} was decreased in the composites as well as C-O vibrations. After the interaction, PE and fillers, vibration which reveals unsaturated C=C bond founding in styrene and mostly seen at 910 cm^{-1} for PE, disappeared in the PE-S, PE-B, and PE-Q composites that this phenomenon revealed that polymerization and curing were carried out [20, 28]. Besides, neither asymmetric nor symmetric Si-O vibrations were specifically seen in the spectra for the PE-B, PE-Q, and PE-S composites. Those vibrations probably overlapped with the C-O vibrations between 1150 cm-1-850 cm-1[19].

3.2. Thermal Characterization

3.2.1. Thermogravimetric Analysis Thermal Conductivity

The thermogravimetric analysis (TGA) and it's derivative (DTG) indicate the starting and end temperatures of thermal degradation, as well as the number and content of the steps involved in the thermal degradation temperature related to the composites, are given in Figure 5. Also, the 10%, 50% weight loss, the decomposition temperature, and residue (%) are summarized in Table 3.

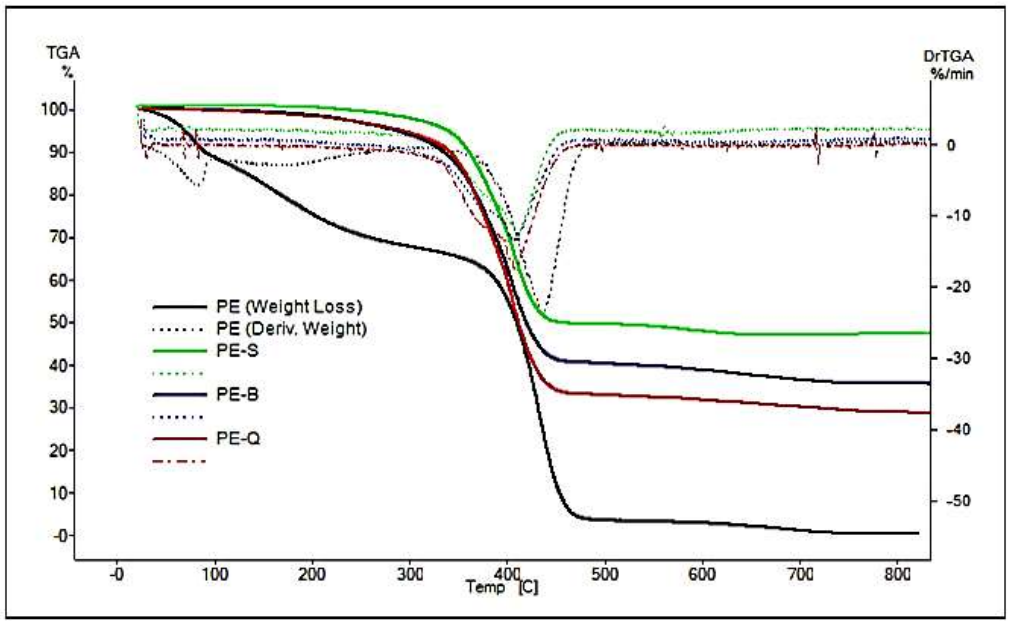

Figure 5. Thermogravimetric analysis results of the PE, PE-S, PE-B, and PE-Q composites.

Table 3. Thermal degradation temperature values of the composites.

Samples	$T_{10\%}$ (°C)	$T_{50\%}$ (°C)	*Td* (°C)	Residue (%)
PE	92.1	404.1	388.5	0.2
PE-S	361.2	448.2	351.1	46.01
PE-B	336.6	421.4	343.9	35.8
PE-Q	343.4	407.9	348.3	28.9

In Figure 5, the PE-S, PE-B, and PE-Q composites revealed mostly similar thermal degradation temperature trend except for the PE. When investigated the T10% values, the thermal stability of the composites increased with the fillers that the PE-S, PE-B, and PE-Q composites exhibited higher thermal stability compared to the neat PE with an enhanced decomposition temperature about 361.2, 336.6, and 343.4 °C, respectively. Also, a similar trend continued with a T50% degradation temperature that degradation was carried out in the 448.2, 421.4, and 407.9 °C for PE-S, PE-B, and PE-Q, respectively. However, PE-B degraded at a lower temperature compared to PE-S and PE-Q. It means that basalt caused lower heat transfer, thus diminishing the thermostability and leading to earlier degradation.

In contrary to Shimazaki et al, organic fillers used in that study caused higher thermostability [21]. It means that filler's structure influenced thermal stability that as organic-based fibrils decreased the thermal stability whereas minerals having inorganic chemical structure enabled higher thermostability [22-25]. This

circumstance can be explained with the organic cellulose fillers enabled chain mobility of the polymer within the composite whereas inorganic fillers restricted chain mobility in the matrix on the long-range [26]. When investigated the derivative curves, two thermal degradations were seen for PE. It was seen only PE in the first thermal degradation. Then, in the second degradation, PE-B was degraded firstly. However, the highest thermal degradation temperature was seen in PE.

Besides, solid residue is higher in the PE up to 800 °C. This is ascribed in inorganic particles. Inorganic particles comprised of a variety of metals and oxides. These metals and oxides have a higher melting point compared to organic structures. Thus, when exposed to the temperature, organic-based structures removed faster from the structure whereas inorganic based structures remained in the structure. Therefore, PE-Q, PE-S, PE-B composites having inorganic particles remained in higher value when the solid residue of PE is lowest. Because, the melting point of the basalt mineral is at around 1200 °C whereas the melting point of the quartz and silica is at around 1650 °C and 1400 °C, respectively [29].

3.3. Thermal Conductivity

The results of the thermal conductivity of the produced composites are given in Figure 6 and the statistical analysis related to the thermal conductivity are given in Table 4. The data obtained were analyzed statistically by the variance analysis (ANOVA) and the Duncan test is given in Table 5, and Table 6.

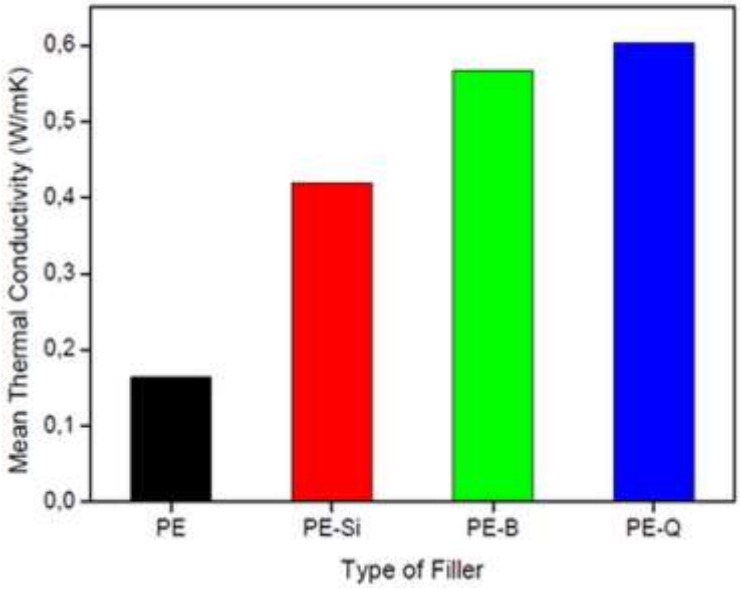

Figure 6. Thermal analysis results of the PE, PE-S, PE-B, and PE-Q composites.

Table 4. Descriptive values of thermal conductivity test results.

Composite type	N	Mean of Thermal Conductivity (W/mK)	Std. Deviation	Std. Error	95% Confidence Interval for Mean		Minimum	Maximum
					Lower Bound	PEper Bound		
PE	4	0.16	0.01291	0.00645	0.1445	0.1855	0.15	0.18
PE-S	4	0.42	0.00816	0.00408	0.4070	0.4330	0.41	0.43
PE-B	4	0.56	0.01500	0.00750	0.5436	0.5914	0.55	0.58
PE-Q	4	0.60	0.02217	0.01109	0.5672	0.6378	0.58	0.63

Table 5. Variance analysis results of thermal conductivity values.

Source of variance	Sum of Squares	Degree of freedom (df)	Mean Square	F	Significance (p≤0.05)
Between GroPEs	0.475	3	0.158	666.281	0.00001
Within GroPEs	0.003	12	0.000		
Total	0.478	15			

Celal Bayar University Journal of Science
Volume 17, Issue 1, 2021, p 79-89
Doi: 10.18466/cbayarfbe.787883

Table 6. Duncan test results of thermal conductivity values.

Type of Filler	N	Different GroPEs (Subset for alpha = 0.05)			
		1	2	3	4
PE	4	0.1650			
PE-S	4		0.4200		
PE-B	4			0.5675	
PE-Q	4				0.6025

Means for groPEs in homogeneous subsets are displayed. a. Uses Harmonic Mean Sample Size = 4.000.

According to the statistical analysis and evaluations of the test results, it was observed that there has been a significant change in the thermal conductivity depends on filler types. The thermal conductivity of the PE composite ascended from 0.16 $Wm^{-1}K^{-1}$ to 0.42 $Wm^{-1}K^{-1}$, which was 2.7 times higher than that of the PE-B composite. However, the highest increment was seen in the PE-Q composite with 0.60 $Wm^{-1}K^{-1}$ that nearly 4 times higher compared to composites obtained from the PE. Also, the thermal conductivity results are agreement with the TGA results that filler-based composites revealed higher thermal conductivity. However, compared to thermal conductivity levels of the PE-Q, PE-S, and PE-B composites, the highest thermal conductivity was seen in the PE-Q composites. It is also known that quartz mineral is higher thermal conductivity property over basalt [26]. It can be concluded that inorganic fillers enabled the higher thermal conductivity results in the thermosetting composites.

3.4. Morphological Characterization

The morphology of the composites was investigated with SEM (Figure 7).

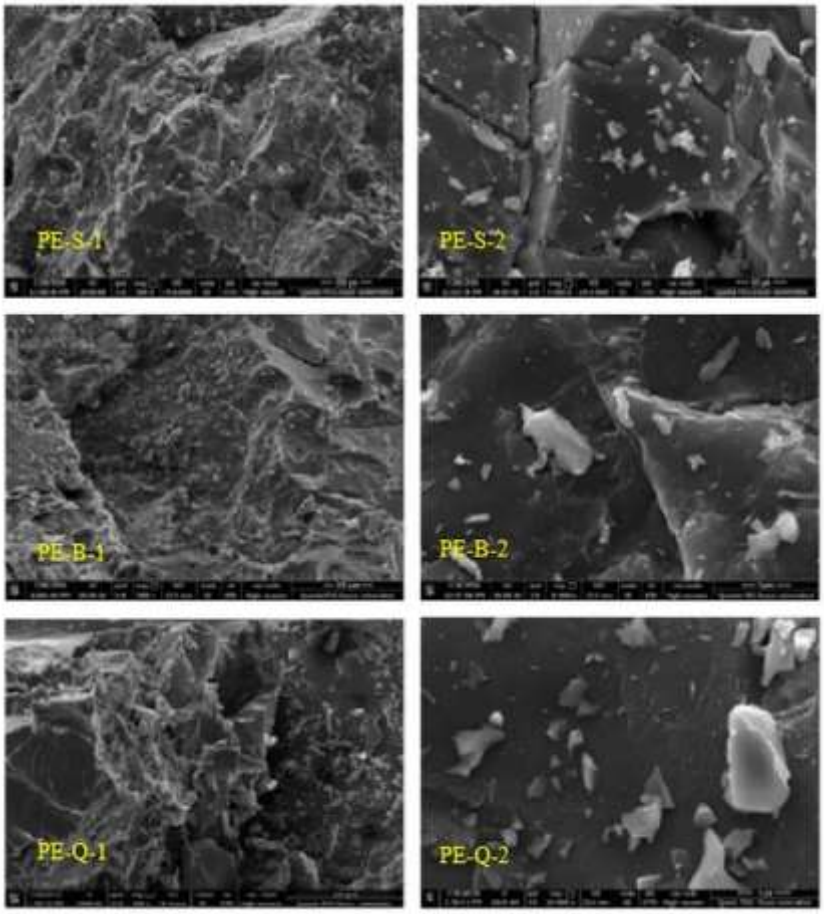

Figure 7. SEM pictures of the PE, PE-S, PE-B, and PE-Q composites.

When investigated SEM images of the composites, all of the fillers mostly dispersed homogeneously in the resin matrix and no agglomeration was observed between resin and fillers since there has been a good adherence between fillers and polyester. Also, there is not considerable cracking and void between surfaces of the fillers and matrix. This probably stems from the lower the dimension of fillers. However, although mostly fillers dispersed in the matrix, silica filler dispersed more homogeneous in the PE matrix than those of fillers and also interacted more effectively with the PE.

It has been also thought that load and energy applied to the composites caused lower fragmentation or cracking. The energy that should be applied to form cracks in the composites was higher since the filler used is low. It was shown that fillers having high hardness carried mostly load that applied. Thanks to this, it protected to matrix against cutting. However, with increasing load, cracking began between interfacial surface and fillers, then fillers eluded from the surface of the matrix towards to sliding side.

3.5. Mechanical Characterization

The results of the compressive strength of the produced composites are given in Figure 8 and the statistical analysis related to the compressive strength are given in Table 7. The data obtained were analyzed statistically by the variance analysis (ANOVA) and the Duncan test is given in Table 8 and Table 9.

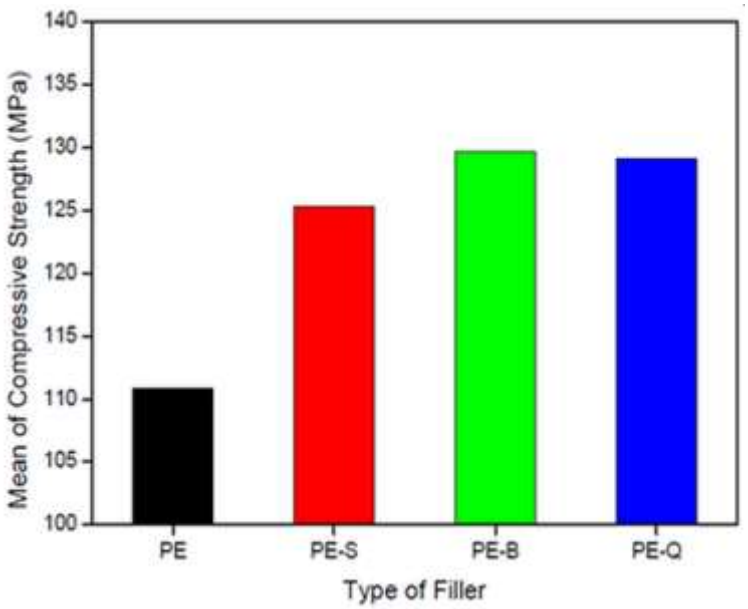

Figure 8. Compressive strength values of the PE, PE-S, PE-B, and PE-Q composites.

Table 7. Descriptive values of compressive strength test results.

Composite type	N	Mean of Compressive Strength (MPa)	Std. Deviation	Std. Error	95% Confidence Interval for Mean		Minimum	Maximum
					Lower Bound	PEper Bound		
PE	4	110.77	1.91551	0.95775	107.72	113.82	108.90	113.40
PE-S	4	125.25	1.06301	0.53151	123.55	126.94	124.40	126.80
PE-B	4	129.72	1.40801	0.70401	127.48	131.96	128.10	131.00
PE-Q	4	129.12	1.60702	0.80351	126.56	131.68	126.90	130.40

I

Table 8. Variance analysis results of compressive strength values.

Source of Variance	Sum of Squares	Degree of freedom (df)	Mean Square	F	Significance (p≤0.05)
Between GroPEs	940.752	3	313.584	133.951	0.00001
Within GroPEs	28.093	12	2.341		
Total	968.844	15			

Table 9. Duncan test results of compressive strength values.

Type of Filler	N	Different Groups (Subset for alpha = 0.05)		
		1	2	3
PE	4	110.77		
PE-S	4		125.25	
PE-B	4			129.12
PE-Q	4			129.72

Means for groPEs in homogeneous subsets are displayed. a. Uses Harmonic Mean Sample Size = 4.000.

According to the statistical analysis and evaluations of the test results, filler types influenced the mechanical results that mechanical properties of the thermosetting composites may vary in comparison to inorganic materials in it.

Compressive strength is of great importance for any structural element. The difference strength values between the groups can be explained by the dependence of the strength of thermosetting composites on various factors such as resin and filling material rates, grain-size distributions, and its heterogeneous structure. It also seemed that composites are prone to fail in bending and the improvement of new composites with improved flexural characteristics is essential.

Fillers improved the compressive strength value of the composites compared to the neat polyester composite. And, the highest compressive strength result was obtained in PE-B composite whereas PE-S revealed lower compressive strength value. This is ascribed in iron oxide and titanium oxide found in the basalt. It is thought that these minerals make this structure strength. However, PE-Q composite value was so close with basalt filled composite.

4. Conclusion

This study reports the effects of silica (S), quartz (Q), and basalt (B) fillers on the chemical, thermal and mechanical properties of PE composites.

Conclusions from this study are as follows:

1. The neat PE and its composites with silica (PE-S), basalt (PE-B), and quartz (PE-Q) were successfully produced with free-radical polymerization and mechanical treatment.
2. After the interaction of filler and PE, minor chemical shifts were observed in obtained composites. The intensity of the basic vibrations of the PE was decreased due to the decrease in the concentration of the resin.
3. Filler based PE composites revealed higher thermostability compared to the neat PE composite due to the inorganic based fillers restricted chain mobility in the matrix on the long-range.
4. All of the fillers were mostly dispersed as homogeneous and no agglomeration was observed that there has also been good adherence between PE and fillers.
5. Filler based PE composites revealed higher thermal conductivity. This phenomenon was an agreement with the TGA results. However, among the filler-based composites, the highest thermal conductivity was seen in the PE-Q composite whereas PE-B revealed close value to it.
6. Filler enabled higher compressive strength over the neat PE. Also, the PE-B composite revealed the highest compressive strength value while the lowest value was observed in the PE-S composite.

This study reveals that the applicability of various filler as a reinforcing agent in polymer composites may alter depending on filler types.

Acknowledgement

The authors gratefully acknowledge the financial support of the Scientific and Technological Research Council of Turkey (TUBITAK). Project Number: 5140058.

Author's Contributions

The authors contributed to the study as follows.

Bayram Poyraz: Investigation, Writing- Original draft preparation, Methodology, Formal analysis

Şevki Eren: Investigation, Writing- Original draft preparation, Methodology, Formal analysis.

Serkan Subaşı: Methodology, Supervision, Project administration.

Ethics

There are no ethical issues after the publication of this manuscript.

References

1. Kalkan, E, Karakışla, MM, Saçak, M. 2018. Polypyrrole and silver particles coated poly (ethylene terephthalate) nonwoven composite for electromagnetic interference shielding. Journal of Composite Materials; 52(10): 1353-1362.

2. Kumar, V, Dev, A, Gupta, A. 2014. Studies of poly (lactic acid) based calcium carbonate nanocomposites. Composites Part B: Engineering; 56: 184-188.

3. Çopuroğlu, M, Şen, M, Keyf, F. 2017. A polymeric nanocomposite system for potential adhesive applications in restorative dentistry. Journal of Adhesion Science and Technology; 31(6): 602-612.

4. Kim, HG. 2002. Dielectric cure monitoring for glass/polyester prepreg composites. Composite Structures; 57(1-4): 91-99.

5. Novak, BM. 1993. Hybrid nanocomposite materials—between inorganic glasses and organic polymers. Advanced Materials; 5(6): 422-433.

6. Ogoshi, T, Itoh, H, Kim, KM, Chujo, Y. 2002. Synthesis of organic− inorganic polymer hybrids having interpenetrating polymer network structure by formation of ruthenium− bipyridyl complex. Macromolecules; 35(2): 334-338.

7. Chen, Y, Iroh, JO. 1999. Synthesis and characterization of polyimide/silica hybrid composites. Chemistry of Materials; 11(5): 1218-1222.

8. Demir, MM, Altın, B, Özçelik, S. 2010. Composites of reactive silica nanoparticles and poly (glycidyl methacrylate) with linear and crosslinked chains by in situ bulk polymerization. Composite Interfaces; 17(9): 831-844.

9. Horath, L. Fundamentals of Materials Science for Technologists: Properties, Testing. and Laboratory Exercises; Waveland Press: 2019.

10. Rothon, R. Particulate-Filled Polymer Composites; iSmithers Rapra Publishing: 2003.

11. Saba, N, Jawaid, M, Asim, M. Recent Advances in Nanoclay/Natural Fibers Hybrid Composites. In: Nanoclay Reinforced Polymer Composites; Springer, 2016; pp 1-28.

12. Mahdi, F, Abbas, H, Khan, A. 2010. Strength characteristics of polymer mortar and concrete using different compositions of resins derived from post-consumer PET bottles. Construction and Building Materials; 24(1): 25-36.

13. Ateş, E, Barnes, S. 2012. The effect of elevated temperature curing treatment on the compression strength of composites with polyester resin matrix and quartz filler. Materials & Design; 34: 435-443.

14. Ateş, E. 2009. Optimization of compression strength by granulometry and change of binder rates in epoxy and polyester resin concrete. Journal of Reinforced Plastics and Composites; 28(2): 235-246.

15. Singh, P, Kaushik, A, Kirandeep. 2006. Mechanical and transport properties of colloidal silica-unsaturated polyester composites. Journal of Reinforced Plastics and Composites; 25(2): 119-140.

16. Fuller WB, Thompson SE. 1907. The laws of proportioning concrete. Journal of Transportation Engineering; 59.

17. ASTM (2012) C579-18. Standard test methods for compressive strength of chemical-resistant mortars. grouts. monolithic surfacings and polymer concretes. ASTM International, USA.

18. Carrillo, F, Colom, X, Sunol, J, Saurina, J. 2004. Structural FTIR analysis and thermal characterisation of lyocell and viscose-type fibres. European Polymer Journal; 40(9): 2229-2234.

19. Heidari, A, Younesi, H, Mehraban, Z. 2009. Removal of Ni (II). Cd (II). and Pb (II) from a ternary aqueous solution by amino functionalized mesoporous and nano mesoporous silica. Chemical Engineering Journal; 153(1-3): 70-79.

20. Chung, CM, Cho, SY, Kim, JG, Oh, SY. 2007. Preparation of unsaturated polyester–silica nanocomposites. Journal of Applied Polymer Science; 106(4): 2442-2447.

21. Shimazaki, Y, et al. 2007. Excellent thermal conductivity of transparent cellulose nanofiber/epoxy resin nanocomposites. Biomacromolecules; 8(9): 2976-2978.

22. Khankrua, R, et al. 2013. Thermal and Mechanical Properties of Biodegradable polyester/silica Nanocomposites. Energy Procedia; 34: 705 – 713.

23. Farhan, AJ. 2020. Characterization the thermal degradation E kinetic of unsaturated polyester and polyester/silica nanoparticles composites by TGA and DSC Analysis. Journal of Advanced Research in Fluid Mechanics and Thermal Sciences; 71(1): 10-20.

24. Carrasco, F, Pages, P. 2008. Thermal degradation and stability of epoxy nanocomposites: influence of montmorillonite content and cure temperature. Polymer Degradation and Stability; 93: 1000-1007.

25. Chrissafis, K, Bikiaris, D. 2011. Can nanoparticles really enhance thermal stability of polymers? Part I: An overview on thermal decomposition of addition polymers. Thermochimica Acta; 523: 1-24.

26. Zhua, J, et al. 2011. Ionic liquid assisted electrospinning of quantum dots/elastomer composite nanofibers. Polymer; 52: 1954-1962.

27. Barry-Macaulay, D, et al. 2013. Thermal conductivity of soils and rocks from the Melbourne (Australia) region. Engineering Geology; 164: 131-138.

28. Cao, X, Lee, LJ. 2003. Control of shrinkage and residual styrene of unsaturated polyester resins cured at low temperatures: I. Effect of curing agents. Polymer; 44: 1893-1902.

29. Baskaran, R, Sarojadevi, M, Vijayakumar, CT. 2010. Mechanical and thermal properties of unsaturated polyester-silica nanocomposites. Nano Science and Nano Technology An Indian journal; 4(1): 1-5.